Supplementary information

Phase separation of p53 precedes aggregation and is affected by oncogenic mutations and ligands

Elaine C. Petronilho[1]*, Murilo M. Pedrote[1]*, Mayra A. Marques[1], Yulli M. Passos[2], Michelle F. Mota[1], Benjamin Jakobus[3], Gileno dos Santos de Sousa[1], Filipe Pereira da Costa[1], Adriani L. Felix, Giulia D. S. Ferretti, Fernando P. Almeida[4], Yraima Cordeiro[2], Tuane C. R. G. Vieira[1], Guilherme A. P. de Oliveira[1]**, Jerson L. Silva[1,]**

[1] Institute of Medical Biochemistry Leopoldo de Meis, National Institute of Science and Technology for Structural Biology and Bioimaging, National Center of Nuclear Magnetic Resonance Jiri Jonas, Federal University of Rio de Janeiro, Rio de Janeiro RJ 21941-901, Brazil.

[2] Faculty of Pharmacy, Federal University of Rio de Janeiro, Rio de Janeiro, Brazil.

[3]Modal Informática Ltda, Almeida Godinho, 19, 304, Rio de Janeiro, RJ 22741-140, Brazil.

[4]National Center for Structural Biology and Bioimaging (CENABIO), Federal University of Rio de Janeiro, Rio de Janeiro RJ 21941-901, Brazil

* Elaine C. Petronilho and Murilo M. Pedrote are equally first authors

** Corresponding authors: Guilherme A. P. de Oliveira and Jerson L. Silva

E-mail: gaugusto@bioqmed.ufrj.br / jerson@bioqmed.ufrj.br

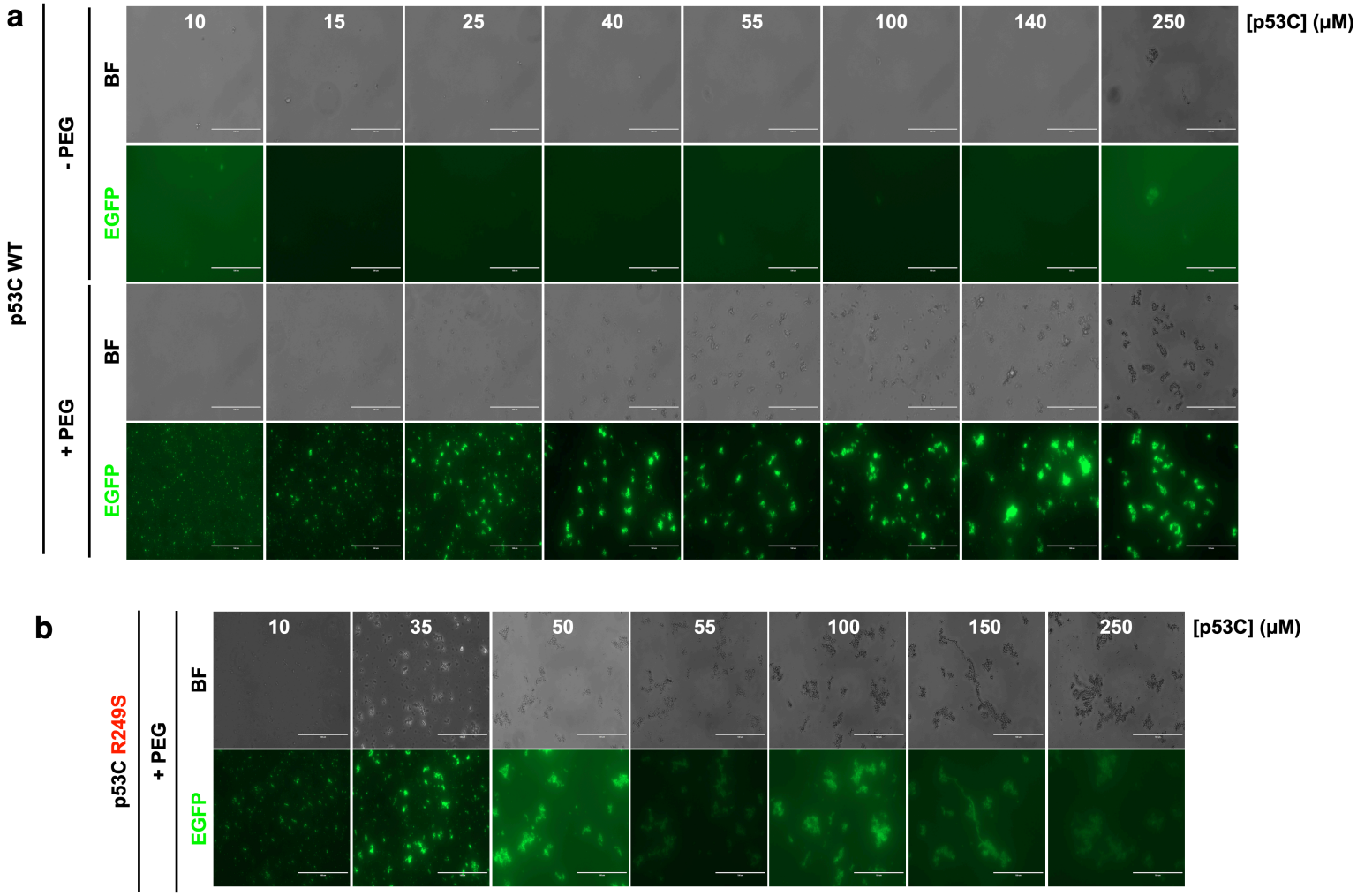

Supplementary Figure 1. Formation of liquid droplets in the presence of PEG and across different concentrations of p53, by DIC and fluorescence microscopy. ***a, b,*** Concentration-induced phase separation of *(a)* WT p53C (10, 15, 25, 40, 55, 100, 140 and 250 μM) and *(b)* R249S p53C (10, 35, 50, 55, 100, 150 and 250 μM) at 4 ºC, in presence and absence of PEG - 4000 (15% w/v). Scale bar, 50 μm.

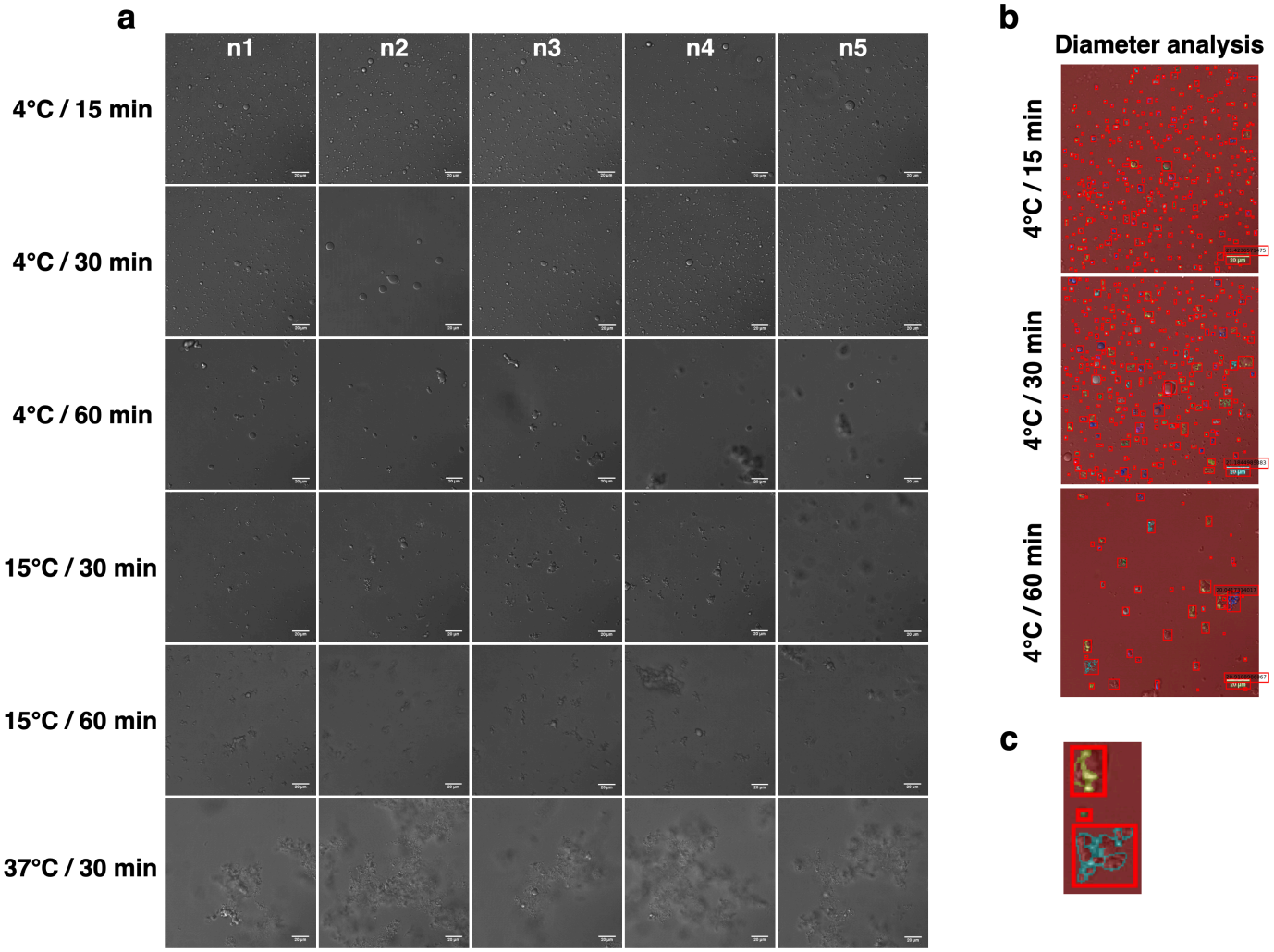

Supplementary Figure 2. DIC microscopy showing that p53C is capable of phase separation. ***a,*** Experimental replicates (n1 to n5) showing the temperature-induced kinetics of WT p53C at 4, 15, and 37°C over time. ***b,*** Automatic droplet detection for diameter analysis at 4 ºC, over time (15, 30 and 60 min). ***c,*** An enlarged image taken from the result set produced by the automatic droplet detection software diameter analysis, showing the formation of spheroids in 60 minutes (Scale bars, 20 μm).

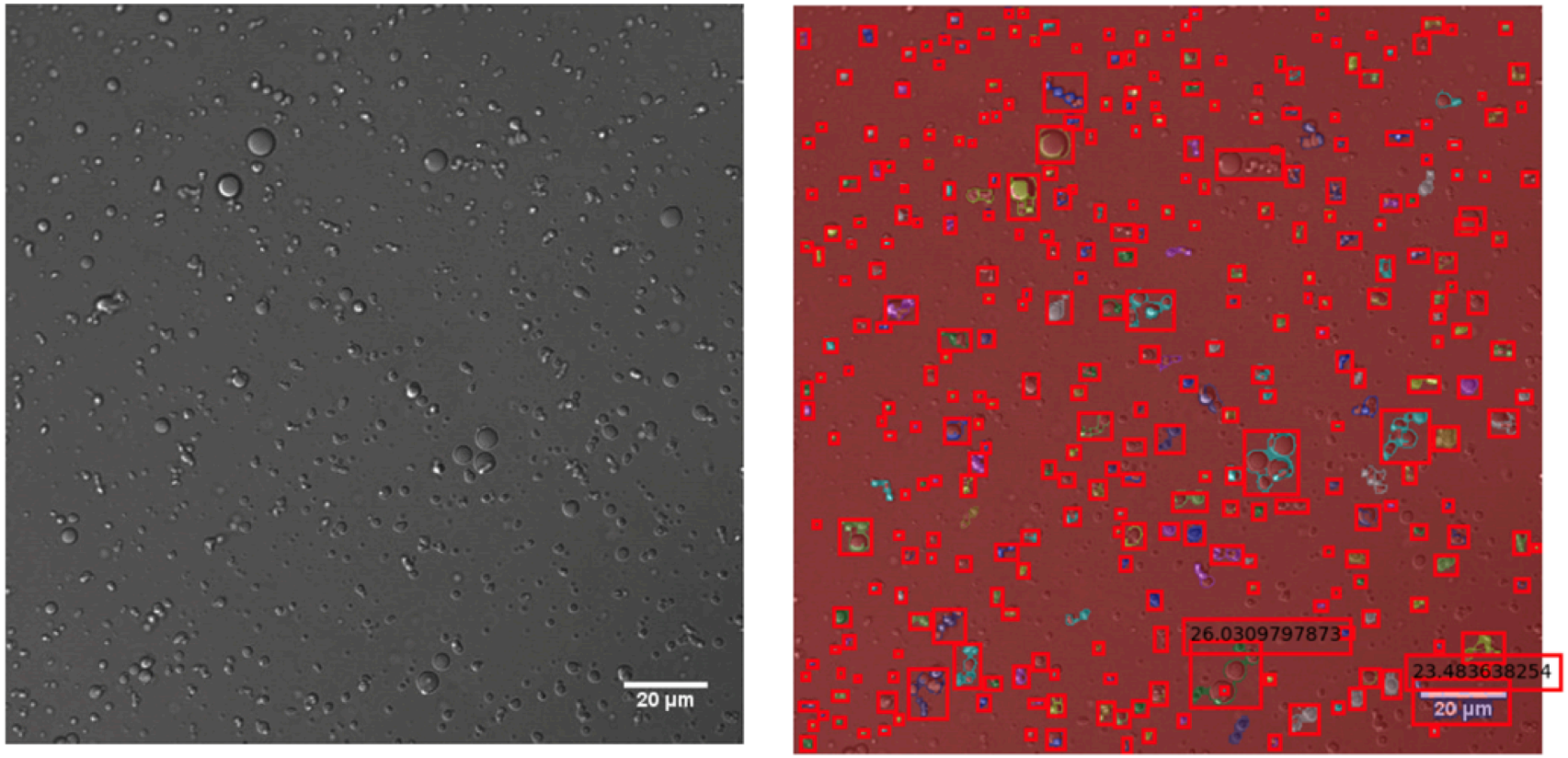

Supplementary Figure 3. A comparison of the original image (left panel) *vs.* the labeled output (right panel). The output contains the axis lengths for outliers. Red squares were drawn around the droplets by the software. We can see by comparing the two images that the vast majority of droplets were detected, barring a few outliers that were more difficult for the software to recognize.

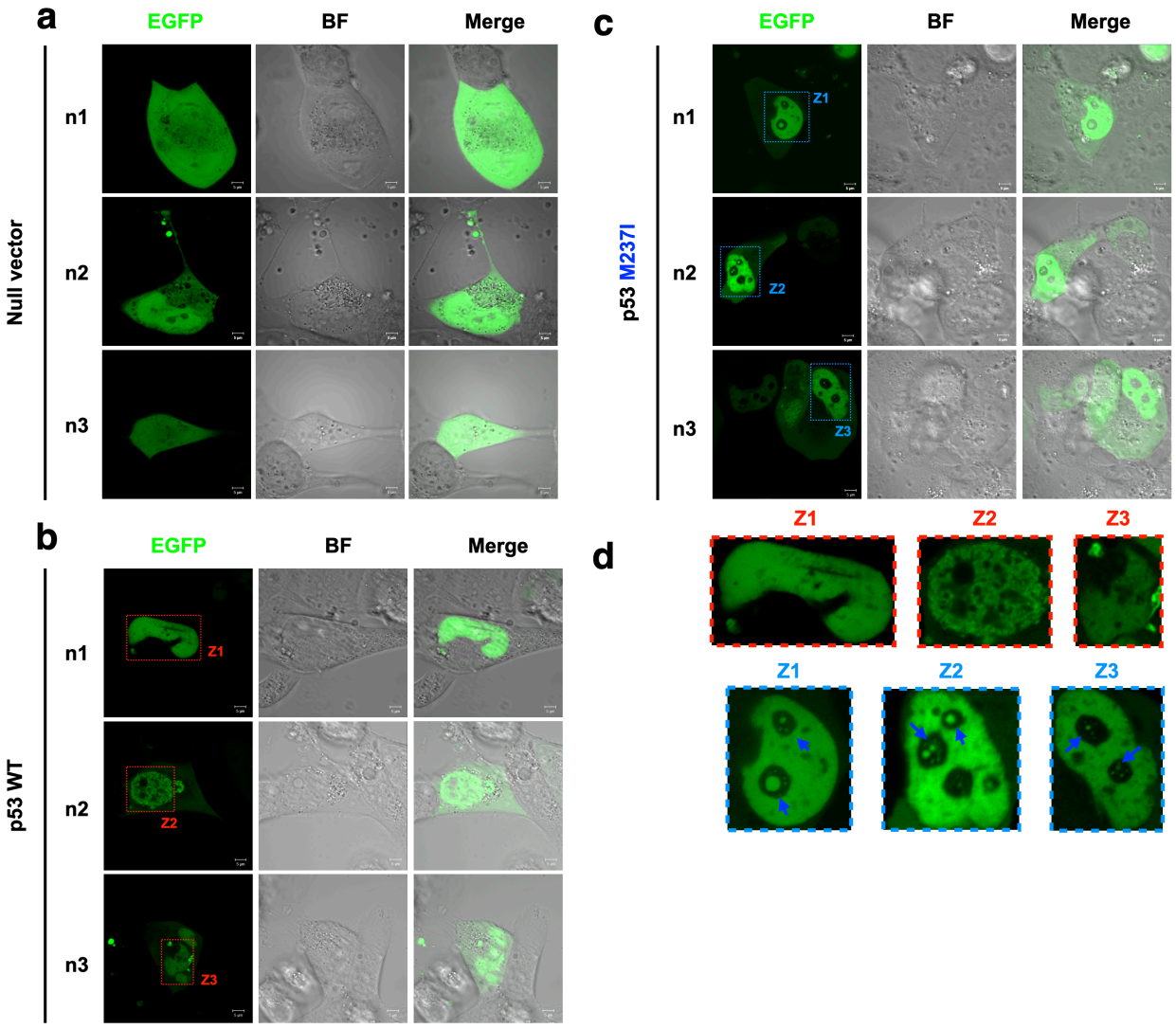

Supplementary Figure 4. Collection of images showing the transfection of the full-length p53. ***a-c***, Confocal images of the fluorescent, bright-field (BF) and the superposition of channels for the *(a)* null vector expressing the EGFP protein, *(b)* WT, and *(c)* M237I p53-transfected H1299 cells. Scale bars, 5 µm. ***d,*** Enlarged images from the result set produced by transfections.

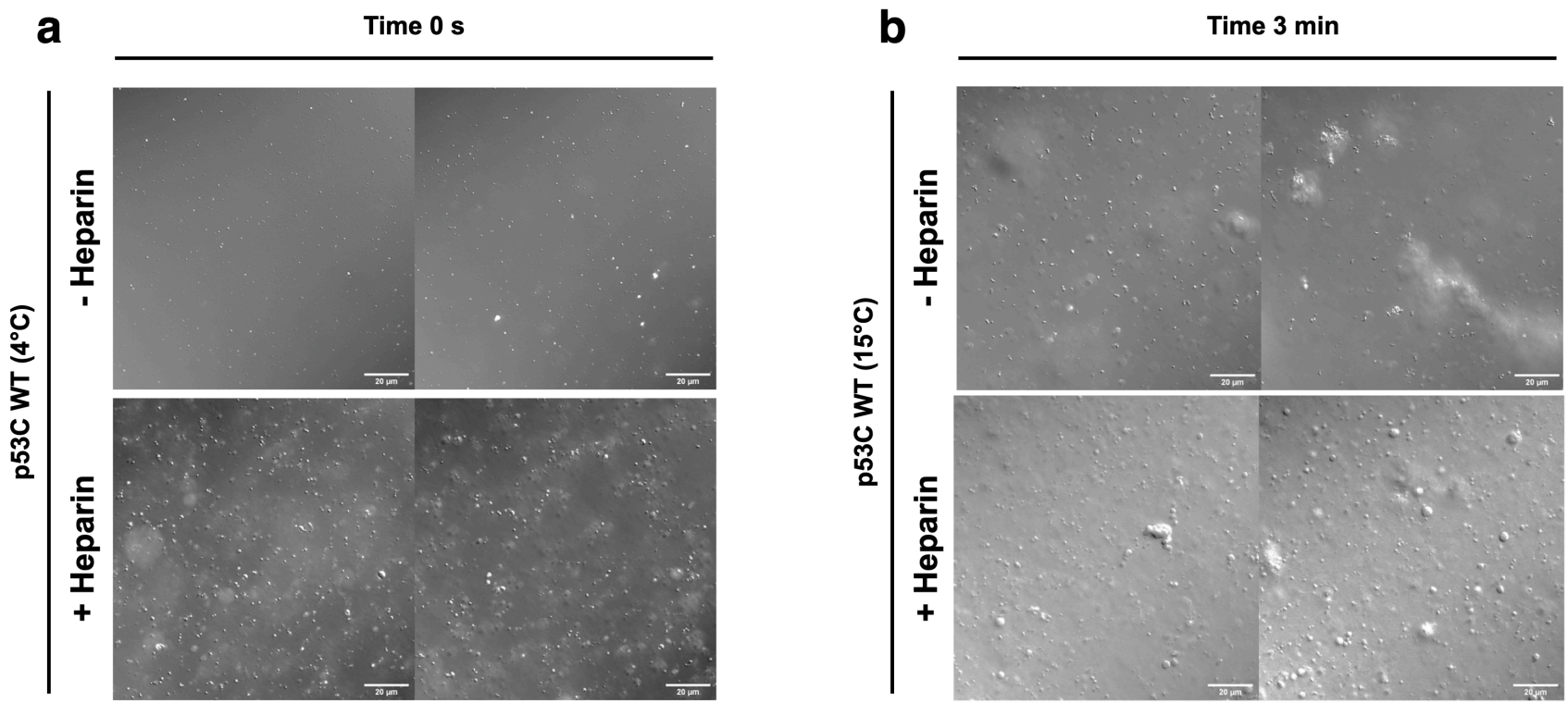

Supplementary Figure 5.
a, b, Bright-field images of WT p53C in the absence (-) and the presence (+) of heparin at *(a)* 4°C Time refers to time at the indicated temperature before PEG and heparin addition.

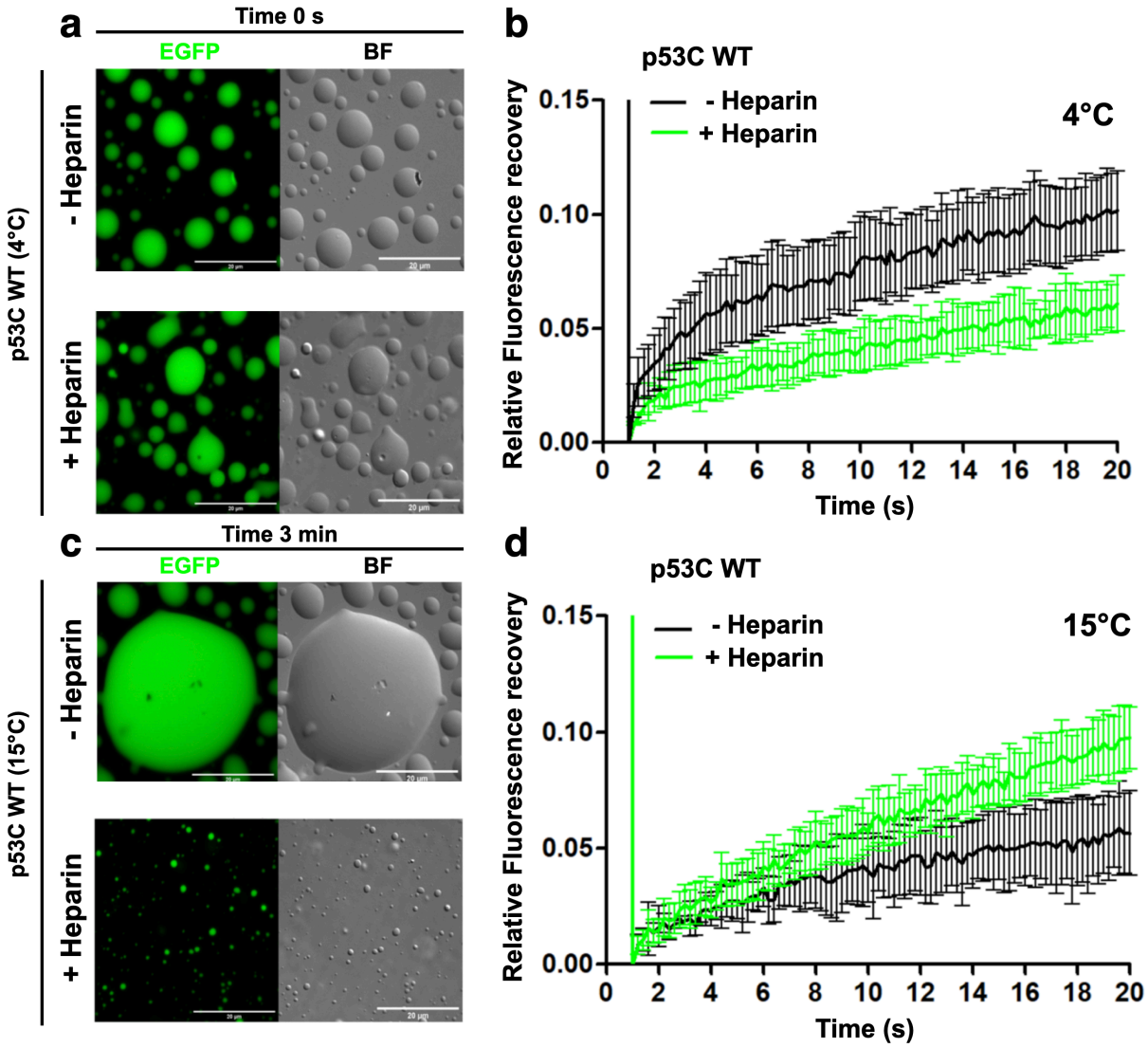

Supplementary Figure 6. Heparin-induced phase separation of WT p53C.
a, c, Fluorescent and bright-field channels of WT p53C in the absence (-) and the presence (+) of heparin at *(a)* 4°C or *(b)* 15°C. Time refers to time at the indicated temperature before PEG addition.
b, d, Line plots showing the fluorescence recovery of WT p53C in the absence (-) and the presence (+) of heparin at *(b)* 4°C and *(d)* 15°C. Data is shown as the avg. ± s.d. of n = 3 measurements.

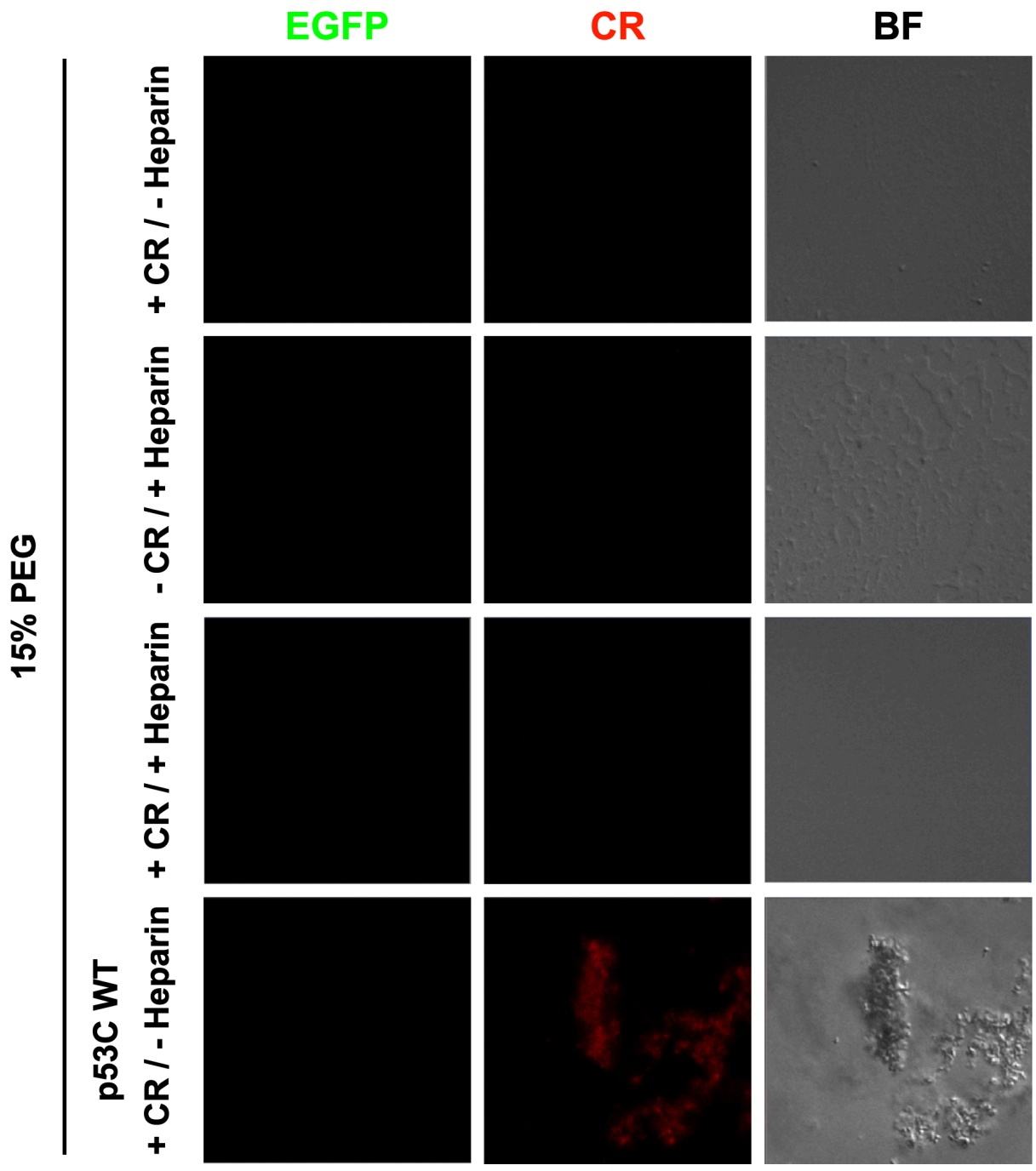

Supplementary Figure 7. CR control experiments.
Collection of DIC images showing fluorescent EGFP, congo red (CR), and bright-field (BF) channels in the absence (-) or the presence (+) of CR and heparin at 4°C right after 15% PEG addition.

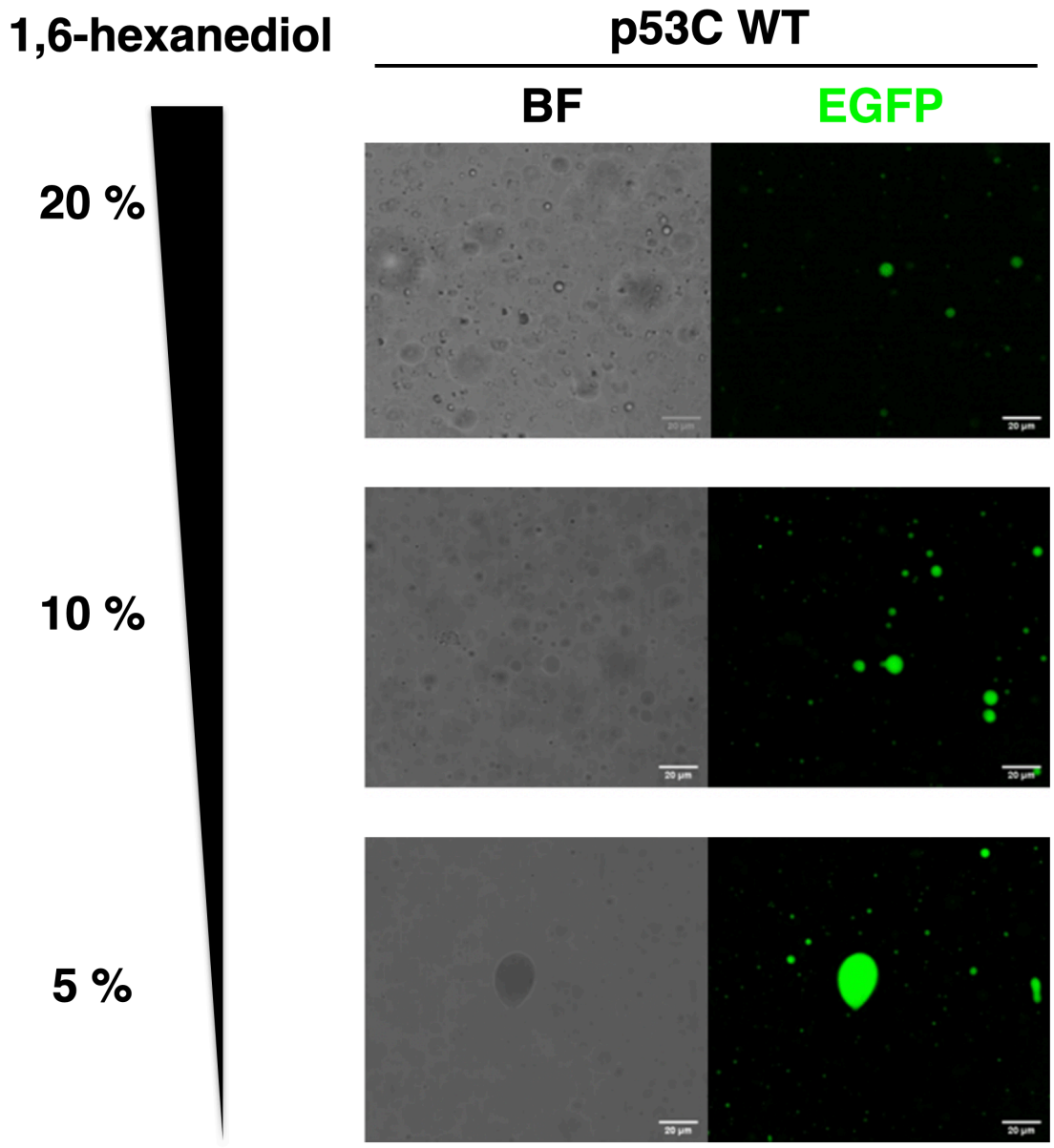

Supplementary Figure 8. 1,6-hexanediol modulates WT p53C phase separation.
Collection of confocal images showing the fluorescent and bright-field channels of WT p53C in the presence of increasing concentrations of 1,6-hexanediol (5, 10, and 20 %). Scale bars, 20 µm.

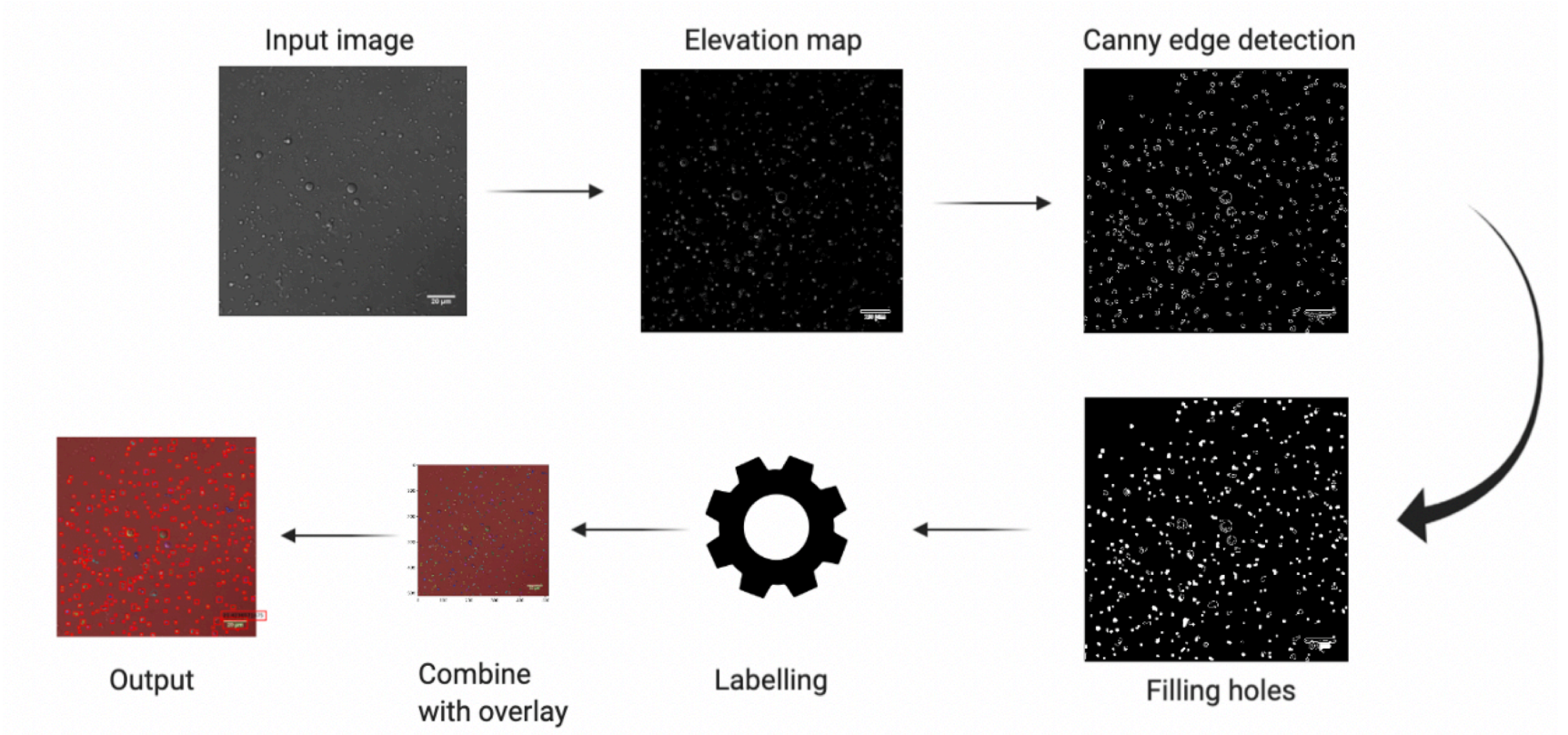

Supplementary Figure 9. An illustration of the steps involved in the automatic droplet detection. Starting with an input image, the software first converted it into a grey scale image, and then produced an elevation map. The canny edge detection algorithm was then applied to this elevation map, before performing binary filling of holes. The resulting image was fed into the labeling mechanism in order to identify the shapes. The labeled image was combined with an overlay to produce the resulting output.

Supplementary Table 1. Results of the automatic droplet detection.

	# Images in category	# Droplets detected	Mean diameter (µm)	Median diameter (µm)
PEG 15 %, 1 hour 4 degrees	8	195	6.47	4.4
PEG 15 %, 1 hour 37 degrees	7	239	4.74	3.54
PEG 15 %, 15 minutes, 4 degrees	15	2179	3.77	2.66
PEG 15 %, 30 minutes, 15 degrees	8	311	5.2	3.94
PEG 15 %, 30 minutes, 37 degrees	6	146	4.95	3.73